Microscopic structure and transitions in xenon multilayer films

James M. Phillips
Department of Physics, University of Missouri–Kansas City, Kansas City, Missouri 64110

John Z. Larese
Department of Chemistry, Brookhaven National Laboratory, Upton, New York 11973
(Received 30 July 1997)

We report a computer simulation analysis of the growth and structural transitions in the first few layers of an adsorbing film. Recent high-resolution adsorption isotherms, heat capacity, and diffraction experiments show remarkable detail in the growth of microscopically thin films. The sharpness of adsorption isotherm steps or the magnitude of their derivative is a measure of the changes in the compressibility of the film during layering. Our computed isothermal compressibilities scale consistently with the corresponding steps in experiments. By these direct observations of equilibrium structures, our study shows these transitions are due to the details of the two-dimensional phase diagram of the top few layers of the film. [S0163-1829(97)01748-7]

INTRODUCTION

Physical adsorption experiments on simple multilayer films continue to pose questions with the occurrence of unexpected transitions and structures. The thermodynamic and microscopic origins of these transitions present a formidable challenge to recent attempts to generalize and model growing films. Our aim has been to understand the structural consequences of the microscopic interactions between adsorbate pairs $u_2(\mathbf{r})$ with each other and with the substrate $u_1(z)$. The relative strengths of these interactions vary widely with the choice of adsorbate and substrate combinations. Experiments and simulations over a variety of systems may well contain the roots to a systematic explanation of the observations.

For films of just a few atomic thicknesses, the adsorbate structures are microscopic assemblies of atoms and molecules whose character is between a purely two-dimensional (2D) and typical 3D systems. In this unusual anisotropic environment, sequences of single layers of film are deposited one by one on small smooth facets of single-crystal solids. This subject has a rich history teaching us valuable lessons in the thermodynamics of physical boundaries. For many decades, basic and applied studies of adsorption[1] have contributed to our understanding of the gas/solid interfaces.[2,3] Advances in the statistical mechanics of adsorption[4] have brought about even broader developments in the fundamentals of interfacial dynamics.

Our efforts are centered on a particular set of experiments that appear to contradict the orthodoxy that has grown around the decades of useful experiments and theoretical efforts. Recent heat-capacity studies[5–12] clearly demonstrated that quite different phase transitions were present in these thin physisorbed films. We have since come to understand that a process of layer-by-layer melting occurs that accounts for many of the observed transitions. There are others that resist clear interpretation. A comprehensive understanding of the microscopic details of transitions driven by the layering mode growth of a film prove to be elusive. Although the seeds of an understanding are clear in the work of Suter and co-workers,[13,14] the impact of the ellipsometry studies of adsorption isotherm by Youn and co-workers[15,16] brought a particular question to the forefront. They named this phenomenon ''reentrant layering.'' The effect of regaining sharpness to adsorption isotherm steps at higher temperatures was then observed by several others.[17–19] The problem was addressed in a formal theory by den Nijs and co-workers[20–22] and by a mean-field approximation[23–25] Our purpose in the sections that follow is to present a more detailed description of these thermodynamic and structural questions. We will report the results from an extensive computer simulation study of these systems and our recent compressibility measurements for xenon on graphite as evidence of our point of view.

FUNDAMENTALS

The contemporary experimental data are of such quality[5–8,11,13–15,18,19,26–29] that the interpretation of subtleties has forced a rethinking of the multilayer growth process. To assist in the interpretation of the experimental detail now available, it is helpful to review the basic structure of multilayer phase diagrams.

Inside the vertical range of the adsorption potential, films grow with increasing chemical potential μ at a constant temperature. Experimental control of chemical potential is achieved by controlling the 3D vapor pressure. The thermodynamic criterion for a film of i layers to coexist with one of $i+1$ layers was derived by Bruch and co-workers[30–32] and applied by Bruch, Unguris, and Webb[30] and Phillips.[33] The positions in the multilayer phase diagram defining a layering transition (an isothermal step) are

$$\mu_i = \mu_{i+1}, \quad \phi_i = \phi_{i+1}. \tag{1}$$

On an isotherm, the increasing chemical potential raises the spreading pressure ϕ stressing the film until a compressional limit[30] is reached. The definition of spreading pressure times the area per molecule is

$$\phi A = \int [p_T(z) - p_{zz}(\mathbf{r})] d\mathbf{r}, \tag{2}$$

where p_T is the transverse component and p_{zz} the vertical component of the pressure tensor.[3] At this limit, it is thermodynamically more favorable for the adsorbing atoms to reside in the next higher layer. Changes in the single-particle vertical distribution function indirectly show the changes in the film's state of stress. The gradient of the adsorption potential $u_1(z)$ weighted with the vertical density $N(z)$ is equal to the zz component of the intermolecular pressure tensor $\mathcal{I}_{zz}$.[3,4] The solution of

$$\frac{\partial \mathcal{I}_{zz}}{\partial z} = -N(z)\,\frac{\partial \mu_1(z)}{\partial z} \tag{3}$$

demonstrates this point.

Heat-capacity experiments measure the change in the entropy of a sample and changes in the isotherm measure isothermal compressibility.[2] The Bruch criterion [Eq. (1)] coupled with the derivative of the adsorption isotherm data gives a firm basis for understanding layering phenomena. The adsorption isotherm is in this way a measure of the isothermal compressibility. We monitor the compressibility (bulk modulus) in our simulations to obtain a relative measure of the sharpness of the isothermal steps. This relationship

$$\kappa_T^{-1} = -kT\left(\frac{\partial \ln p}{\partial A}\right)_T, \tag{4}$$

with A the area per molecule, has since been applied to several different systems.[2,13,14,17,18,34–36] Dash gives an accessible derivation.[2] These relationships [Eqs. (1)–(4)] provide the basis for understanding the nature of simple layering transitions. The numerical derivative of the experimental adsorption is a composite of several ''compressibilities'' of the film. There are several components of the pressure tensor active in the film growth. To the extent that the top of the film is undergoing the most dramatic changes, the experimental compressibility measurement is a sensitive indicator of the 2D phase changes in the growth front of the film.

In the simulations, we monitor the virial theorem and its fluctuations to monitor the 2D pressure and the bulk modulus given by the formulas

$$\frac{\Phi}{\rho kT} = 1 + \frac{3}{2N}\left\langle \sum_{k<j} r_{ij}\,\frac{\partial}{\partial r_{ij}}\left(-\frac{1}{kT}\,u_2(r_{ij})\right)\right\rangle \tag{5}$$

and

$$\begin{aligned}\frac{B}{\rho kT} = \frac{3}{2} + \frac{3}{2}\frac{\Phi}{\rho kT} + \frac{1}{4N}\Bigg(&\left\langle \sum_{i<j} r_{ij}^2\,\frac{\partial^2}{\partial r_{ij}}\left(\frac{1}{kT}\,u_2(r_{ij})\right)\right\rangle \\ &-\left\{\left\langle\left[\sum_{i<j} r_{ij}\,\frac{\partial}{\partial r_{ij}}\left(\frac{1}{kT}\,u_2(r_{ij})\right)\right]^2\right\rangle \right. \\ &\left. -\left\langle\left[\sum_{i<j} r_{ij}\,\frac{\partial}{\partial r_{ij}}\left(\frac{1}{kT}\,u_2(r_{ij})\right)\right]^2\right\rangle\right\}\Bigg),\end{aligned} \tag{6}$$

where ρ is the number density. Equation (6) is important; its change in value from one edge of a 2D coexistence to the other will indicate the relative sharpness of the step. We use this criterion to determine the ''resharpening'' of the fourth step in the 137-K isotherm of xenon on graphite and the third step of the 145-K isotherm. The values of Eq. (6) and the structural distribution functions from the simulations just before and just after a transition is our best determination of the nature of the isotherm profiles.

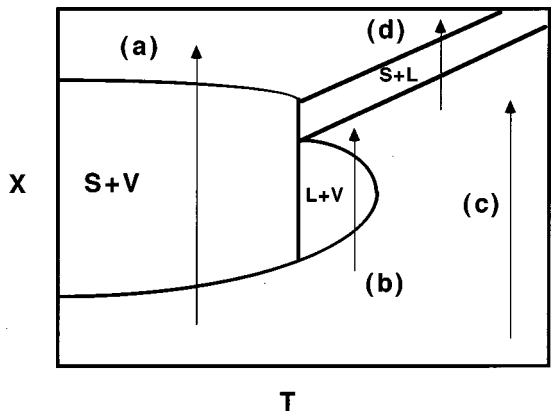

FIG. 1. Schematic representation of a typical 2D phase diagram in coverage (X) with temperature (T). Path (a) represents a solid-on-solid layering that passes through the 2D solid-vapor coexistence region (a sharp step). Path (b) represents the condensation of a layer of liquid by passing through the 2D vapor-liquid coexistence region (a more rounded step). Path (c) represents the layering of a hypercritical fluid by passing above the 2D critical temperature (a ramp). Path (d) represents the ''freezing'' of a liquid layer by passing through the 2D liquid-solid coexistence region (a kink).

We have tried to follow these principles in designing our simulation algorithms and in the analysis of the experimental data. In the adsorption of microscopically thin films, a strong substrate holding potential drives the growing adsorbate elastically through a sequence of compressional limits (coexistence regions). The phase at the top of the film is dependent upon the temperature and the values of the layer triple and critical points.

ISOTHERM PROFILES

In the first four to five layers closest to the substrate, the phases of the topmost layer of the film may resemble those of a monolayer. Within this growth region there are four basic events that can occur during an adsorption isotherm experiment. These intralayer transitions are the analogous to those observed in monolayer systems. This pattern persists as long as the film thickness remains in the effective range of the substrate holding potential. Beyond these several layers this 2D topology of the phase diagram is not experimentally resolvable. Figure 1 is a schematic diagram (coverage with temperature) of a typical 2D system. These phase diagrams are topologically the same as the density versus temperature plot from a traditional 3D equation of state. In the traditional 3D phase diagram (pressure, volume, and temperature) the solid-liquid coexistence region rises in slope with pressure (or chemical potential). The slopes of the lines representing these regions are given by the Maxwell relation

$$\left(\frac{\partial \mu}{\partial T}\right)_N = -\left(\frac{\partial S}{\partial N}\right)_T. \tag{7}$$

The greater the change in the state of disorder in a given transition, the steeper the slope of the corresponding line in

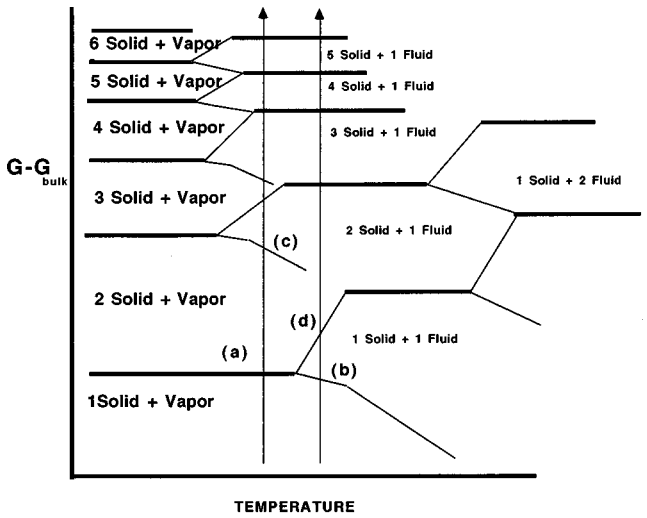

FIG. 2. Typical representation of rare gas on graphite multilayer phase diagram in Gibbs free energy (chemical potential) with temperature. The crossings $(a)-(d)$ are the same as in Fig. 1. The lower-temperature vertical isothermal path shows the sequence of transitions followed by our Xe/graphite study at $T=137$ K. The higher-temperature path shows the sequence of transitions seen in our study of the $T=145$ K isotherm.

the phase diagram. In Fig. 2 the slope of the lines for paths $(a)-(d)$ illustrate this relationship in terms of the entropy S (disorder) of the transition associated with that path. There is a clear theme to the structure of vapor pressure isotherms illustrated in many of the early monolayer studies.[1,37,38] At low temperatures, path (a) crosses the 2D-solid–2D-vapor sublimation region of the layer. This usually results in a sharp isotherm step. In this process, the 3D vapor is adsorbing onto the top of the film and a coexistence condition exists ending in the growth of a solid layer to the top of the film. When the temperature exceeds the 2D triple point for that layer, path (b) crosses the 2D liquid-vapor region. In this coexistence region (condensation), the layering is in the form of a 2D liquid. The pattern of the isotherm is a progressively more rounded step. The length of the vertical rise is less than in path (a). Path (c) follows an isotherm at a higher temperature than the 2D critical point. The layer deposition is in the form of a 2D hypercritical fluid, i.e., there is no 2D condensation within the growth front. The form of the isotherm profile is more of a ramp. There may be an inflection point, but there will not be a vertical portion to the isotherm. The mobile fluid does not condense but remains a single phase right up to the 2D-liquid–2D-solid coexistence line. Path (d) produces a short kink in the isotherm. The dense liquid freezes under the increasing spreading pressure (Clausius-Clapeyron equation). These features are all quite well defined by the monolayer data given in the early papers in the contemporary era of physisorption.[37–39] The thermodynamic[14] and the diffraction experiments[13] of Suter and co-workers on the krypton/graphite system and the work of Larese and co-workers[26,28,29] on the argon/graphite system confirm quite clearly this basic pictures of events. Insofar as experimental conditions allow, *an adsorption isotherm cutting across the multilayer phase diagram will have a profile made up of a sequence of these four possible features (step, rounded step, ramp, and kink).* It is also important to note that a remnant of this pattern persists at high temperatures for the ith layer in a film of $i+1$ layers. The top of the film is a highly mobile dense vapor that with sufficiently increased coverage solidifies the buried ith layer of the adsorbate. Our simulations show that the interfacial atoms are quite mobile vertically as well as horizontally. The horizontal nature of the experimental lines [see Eq. (5)] is ample evidence that the terminal phase of the layering tier (ith) is *solid*. To our knowledge, experimental data have not yet resolved the higher-temperature sequence of layering transitions where the layering tier is buried under two or more layers of fluid. Within a given coexistence region the compressibility of the layering tier remains very large until the denser phase's boundary is reached. At this boundary, the large and sudden change in the compressibility occurs. Hence the step in the isotherm appears. The larger the density difference between the two 2D phases (vapor/liquid, liquid/solid, or vapor/solid), the larger the compressibility change and the higher the vertical portion of the isothermal step.

Our primary attention has been in the first few layers, which are strongly affected by the substrate-induced stress. The lattice-gas or restricted solid-on-solid (RSOS) model is only qualitative in this narrow region because it cannot have a compressibility. Its area per atom does not change with increasing spreading pressure. Spreading pressure and chemical potential are the thermodynamic variables defining layer coexistence [Eq. (1)].

Above we described the intralayer phases and transitions insofar as refined experiments can distinguish. As the film thickens, the single-layer portion of the phase diagram may be preempted by capillary condensation of bulk adsorbate if the substrate is less than perfect. Even without the onset of capillary condensation, the thicker the film becomes the closer chemical potential approaches that of the bulk value for the adsorbate. More and more layer coexistence regions are crowded into a narrowing range of the chemical potential. In experiments and simulations it becomes increasingly harder to determine the 2D coexistence regions. Additional difficulties arise when the temperature is raised; desorption makes the control or measurement of coverage difficult. Based on numerous experiments,[6,7,11,13–16,18,19,27–29,40,41] we show a schematic of a typical multilayer phase diagram (see Fig. 2). For rare-gas adsorbates and graphite substrates, these systems scale to very similar multilayer phase diagrams quite well with corresponding states. We will make our general statements relative to this picture. None of the experiments are able to cover such an extensive range of variables. This represents a qualitative model of what might be expected if one or more experimental difficulties did not prove limiting. The xenon data[16,41] are perhaps the most resolved and the system we will refer to in the detailed discussion of the our simulation results. In comparing Figs. 1 and 2, notice that in Fig. 2 a single-layer region is a side view of the 2D diagram depicted in Fig. 1. The paths are lettered the same in both. Path (a) is crossing the coexistence (layer sublimation line) for a sharp vertical step. Path (b) is the 2D liquid-vapor coexistence region (the slightly rounded step) and path (c) is the deposition of a layer of hypercritical fluid (ramp). Path (d) is the kink produced when a deposited liquid layer freezes under compression. Note the situation at higher tem-

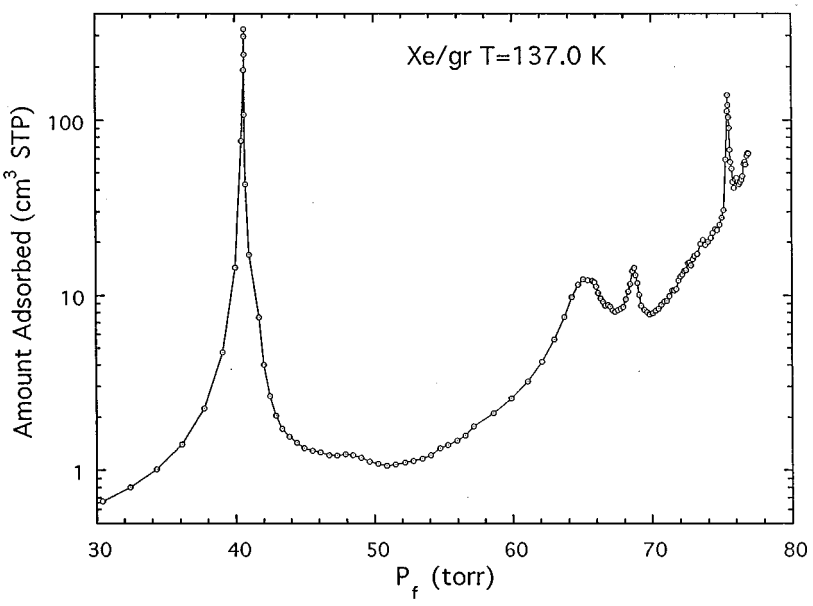

FIG. 3. Plot of the derivative of the experimental 137-K isotherm reported by Zhang and Larese (Ref. 41). The changes in this composite of the isothermal compressibility are shown by the peaks in the plot as the film goes through the layering sequence (growth). The higher and sharper the peak, the more vertical and greater the step observed in the adsorption isotherm (Refs. 16 and 41). The data show first the very sharp step of the solid second layer followed by the condensation of the rounded step of the liquid third layer. This is followed quickly by the freezing of the third layer under a liquid fourth. The reappearance of the sharp step is the freezing of the fourth step under an additional fifth layer of liquid.

peratures, where the top of the film is more than one level of fluid and the part under this liquid growth front solidifies into a solid layer. The film has ascending columns of solid, one liquid layer, two liquid layers, and so on. In fact, it is clear in the data[29,41,42] that the accommodation region between the solid-on-solid column at lower temperatures and the one layer of the liquid-on-solid column slopes backward in the low-temperature direction. This becomes crucial to the understanding of what is going on in the ''reentrant layering'' or ''resharpening of isothermal steps'' process. The resharpening behavior is quite pronounced in the 135-K and higher isotherms for xenon. Figure 3 plots the numerical derivative of the 137-K isotherm by Zhang and Larese.[41] The five features are in sequence: the second-layer sharp step, the third-layer fluid, the freezing of the third layer, and the ramp of a composite fourth and fifth layers of dense fluid and the freezing (resharpened step) of the fourth layer under the fluid fifth. The return of the path-(a) type crossings (sharp steps) for higher layers under a layer of fluid is observed in the higher narrow peak in the compressibility. This is in the ''resharpened'' path of Fig. 2. The changes in the film stress from the simulation results correspond to the compressibility measurements from the experimental adsorption isotherms. In the 137-K isotherm of xenon on graphite by Youn, Meng, and Hess,[16] the first sharp step is the coexistence of solid layer 2 forming on solid layer 1. This is followed by a rounded step of a fluid coexistence region in layer 3, i.e., layer 3 goes down as a 2D fluid, which is followed immediately by a ''kink'' showing the freezing of the third layer by compression. A ramp is next, where additional fluid is deposited. A solid layer 4 forms under the liquid growth front with a sharper layering transition. A series of additional identical steps form in rapid succession for layers 5 and 6. Beyond this the chemical potential is so close to the bulk that the experiments have difficulty following the growth. Figure 4 is the plot of the 2D virial [Eq. (5)] for the 137-K isotherm. The sequence of changes in the transverse stress in the sample show how the film is experiencing different levels of compressibility. Any local maximum is qualitative since we are not able to sit perfectly atop a given transition. The location of the peaks or mounds in coverage is quantitative within the limits of the finite-size effects of our simulations.

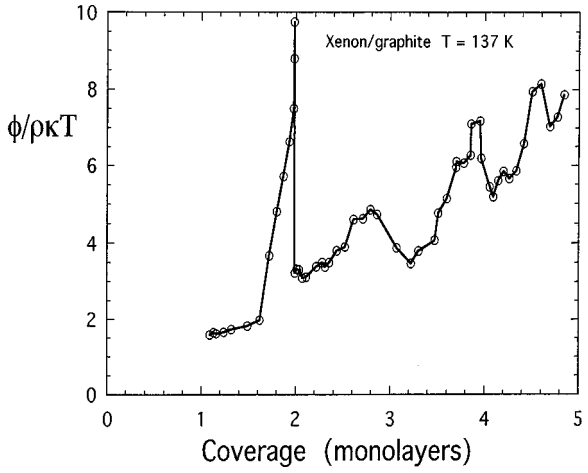

FIG. 4. Results of the dimensionless spreading pressure with coverage from our simulations [Eq. (5)]. Consistent with the Bruch layering criterion (1), the lateral stress builds up in the film as a layer is completely populated and the filling of the next layer begins. The location in coverage of the peaks is quantitative, but the maxima of the peaks are qualitative. It is not possible to find the exact number of atoms in the finite system that produces the maximum of the experimental thermodynamic limit.

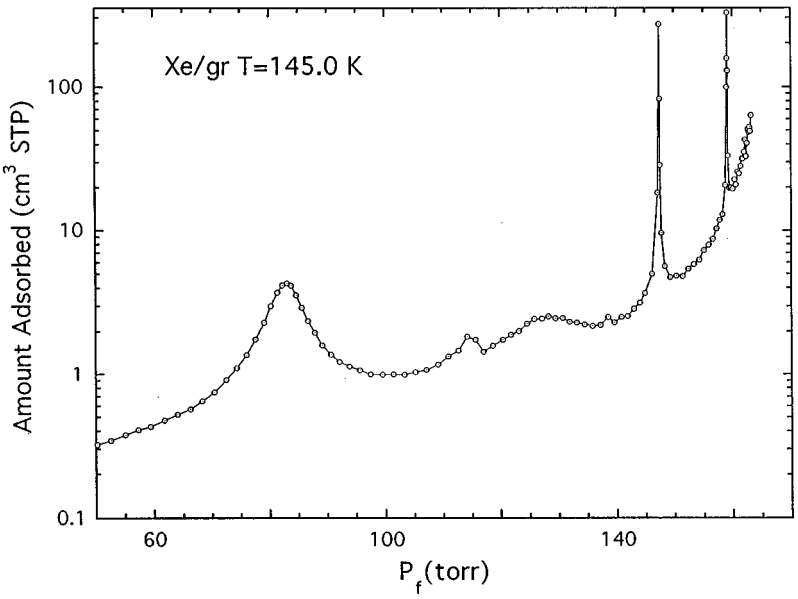

FIG. 5. Same as experimental data in Fig. 3 except for $T=145$ K. At this temperature the second layer is initially a 2D liquid in contrast to the same peak at 137 K. The reappearance of the sharp peaks occurs one layer thinner than in the 137-K isotherm. Again, they become solid under an additional layer of liquid.

Figure 5 is the numerical derivative of the 145-K isotherm by Zhang and Larese. The features in sequence are the second layer of liquid, the freezing of the second layer, the deposition of the third and partial fourth layers of dense fluid, and the freezing (resharpening) of the third layer under the fourth fluid. The additional peaks are the resharpened fourth under the fifth fluid and the resharpened fifth under the sixth fluid. Our simulation results and the scattering data of Zhang and Larese[41] are consistent with theses interpretations of the data.

RESULTS

Our Monte Carlo simulation methods are describe in previous papers,[17] so we omit the description. Although many different thermodynamic conditions could be used to demonstrate the structural and thermodynamic changes occurring in a growing film, we base our explanation of these events on certain pivotal xenon-on-graphite isotherms. These adsorption experiments show all of the possible layering paths available to the film in the first few layers of growth above the substrate. Our reasons for this choice are due to the very high resolution of the experimental data. The xenon-on-graphite isotherms taken by Youn, Meng, and Hess[42] and by Zhang and Larese[41] are of such quality that the subtleties needed are clearly present. In the same paper[41] Zhang and Larese present x-ray-diffraction profiles detailing the structures of these films. In this paper, we present the microscopic nature of the sequence of ''steps'' observed in experiments.

The 137-K isotherm in Fig. 3 (Refs. 41 and 42) shows a sharp step for the growth of the second layer upon the first followed by a rounded rise as the third layer condenses on the top of the film. This rounded step is closely followed by a small sharp rise or kink. Then a series of lower but quite sharp vertical steps reappear, which with Youn and Hess's argon experiments[15] would have seemed to contradict conventional wisdom on layering transitions. The same unusual reappearance occurs in all of the higher-temperature isotherms up through 150 K.[41] The 145-K isotherm is very interesting in that this sequence of events occurs for a film one layer thinner. The numerical derivative of the adsorption isotherms is a measure of the changes in a composite isothermal compressibility or its reciprocal, bulk modulus [Eq. (6)]. These changes reflect, in part, the nature of the coexistence region given by the isotherm step. Figure 3 is a plot of the numerical derivative of the 137-K isotherm taken by Zhang and Larese.[41] Figure 4 shows the results of our simulations for the 2D virial [Eq. (5)] for the 137-K isotherm. Figure 5 is the plot of the numerical derivative for the 145-K isotherm measured by Zhang and Larese.[41] These plots are a series of peaks whose height and sharpness reflect the changes in the compressibility of the film as it grows.

Our computer simulations for these same conditions give a clear picture of the nature of the film before and after leaving these transition coverages. The first large peak in Fig. 3 is over two decades in height and results from the first sharp step in the experimental isotherm. Figure 6 is a plot of the 2D pair distribution functions of each layer in the simulation as the second layer of the film passes through its own 2D solid-vapor coexistence region. The change in the dimensionless bulk modulus $B/\rho kT$ taken in the simulation is 95 for this step. It should be noted that we needed to add atoms to the simulation until there were enough to virtually complete the second layer before the solid locked in. As the film further thickens, the third layer is adsorbed on top of the now two layers of solid. The 2D phase on top of the film is now a fluid. Figure 7 shows that the third layer is fluid and snapshots of the top layer show the fluid to be largely condensed clusters suggesting a 2D liquid-vapor coexistence. The change in the ensemble-averaged bulk modulus for the plateaus in this region is 15 followed by a 12. This layer passes through a 2D liquid-solid region at only $\frac{3}{4}$ of a layer (see Fig. 7). The dense fluid freezes near the coverage $X=2.75$ ML.

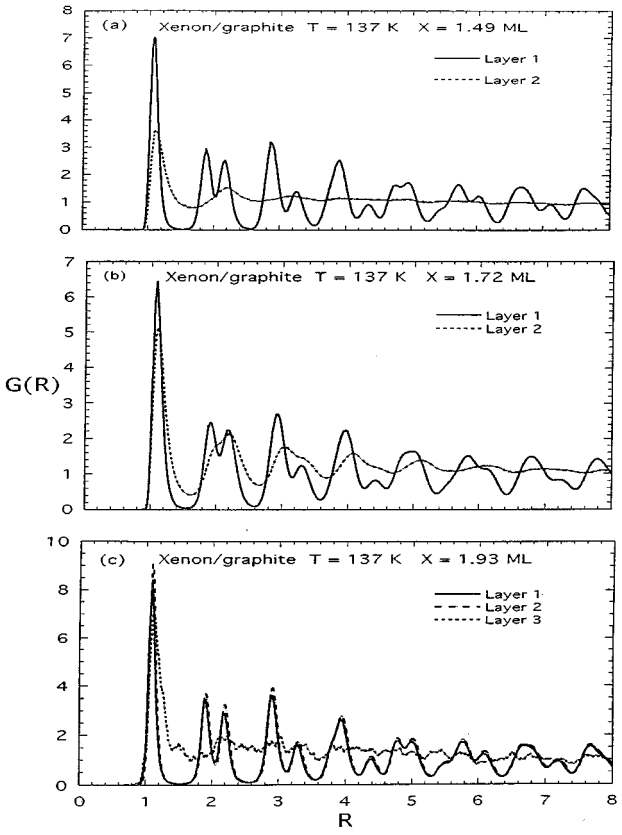

FIG. 6. Plots of our simulation results for the 2D pair distribution function for the individual layers in the film. (a)–(c) follow the film through growth of the second layer solid at 137 K. The change in the computed bulk modulus (6) from the film shown in (b) to (c) is 95.

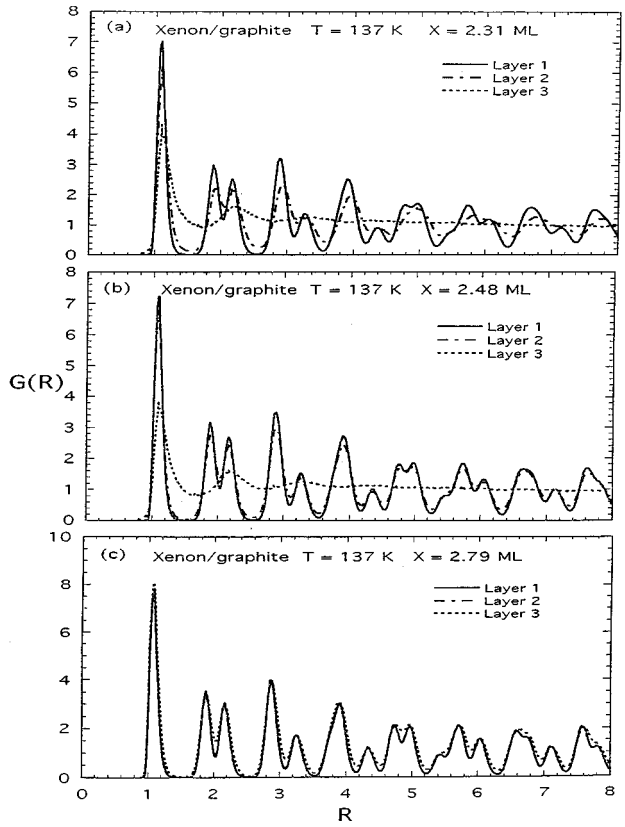

FIG. 7. Same basic plots of the simulation results of the 137-K isotherm. This follows the film from the (Fig. 2) 2 solid+vapor to the 2 solid+fluid region and in (c) the films has just passed into the 3 solid+vapor regions. From the state in Fig. 6(c) up to near Fig. 8(c) the bulk modulus has changed [Eq. (6)] by 15. Passing through the state shown in Fig. 8(c), the bulk modulus has changed by 12. This is quite a contrast to the 95 for layer 2. Note the pair of small more rounded peaks in Fig. 3.

In the isotherms, this is a small kink; in the compressibility shown in Fig. 3 it is a low but sharp peak. This is quite different from the second-layer growth as one might expect from the monolayer phase diagrams given by Thomy and Duval[38,39] and by Larher[37] based entirely on vapor-pressure isotherms. The three layers of solid are topped by an increasingly thick surface of fluid until the film coverage is more than 3.7 ML (Fig. 8). The top of the film is now farther from the substrate and relies upon its own fluid density for compression into a solid rather than compression of the strong substrate potential.

Only when the film is nearing five layers (Fig. 8) does the fourth full layer condense to a solid. This ''freezing'' or solid layering at the top of the film has not gone through a 2D liquid-solid region. The change in the bulk modulus across the fourth tier layering is 59. Its positioning in chemical potential, relative magnitude, and amount of adsorbed material is consistent with Fig. 3 and the fourth step of Fig. 3 found by Youn, Meng, and Hess.[42]

Figure 5 shows the experimental data for the 145-K isotherm. The second layer is initially a fluid (Fig. 9). It becomes a 2D solid at $2\frac{1}{2}$ layers. Figure 10 show the resharpening of the third layer (one layer thinner than at 137 K) under the fluid in the fourth layer. Again, the structure is clear and the bulk modulus change is 32 from the simulations [Eq. (6)]. The compressibility changes is sharp but not as severe in density change as that found at the lower temperatures.

DISCUSSION

The relative magnitudes of the changes in bulk modulus in the simulations for the 137-K and 145-K isotherms are in the proper proportions. The first sharp step in the 137-K isotherm has a difference across the transition of 95, where the deposition of the fluid and its freezing are an order of magnitude less (15 and 12, respectively). The resharpened step (or peak in the derivative) is only 59 in the 137-K fourth layer and 32 in the third layer for the 145-K isotherm. These magnitudes are approximate, but quite consistent with the experiments and the proposed description we offer.

We have computed the equilibrium properties for a number of temperatures and many decades of closely spaced coverages. Our discussion is, however, limited to two temperatures 137 and 145 K because the experimental isotherms [16,41] for these temperatures are crucial to the controversy surrounding the so-named reentrant layering phenomena. These two experimental isotherms contain all of the possible condensations seen in the growth of simple solid inert gas films. We reduce the size of our report but keep all of the unique features in selecting these two particular isotherms. Our

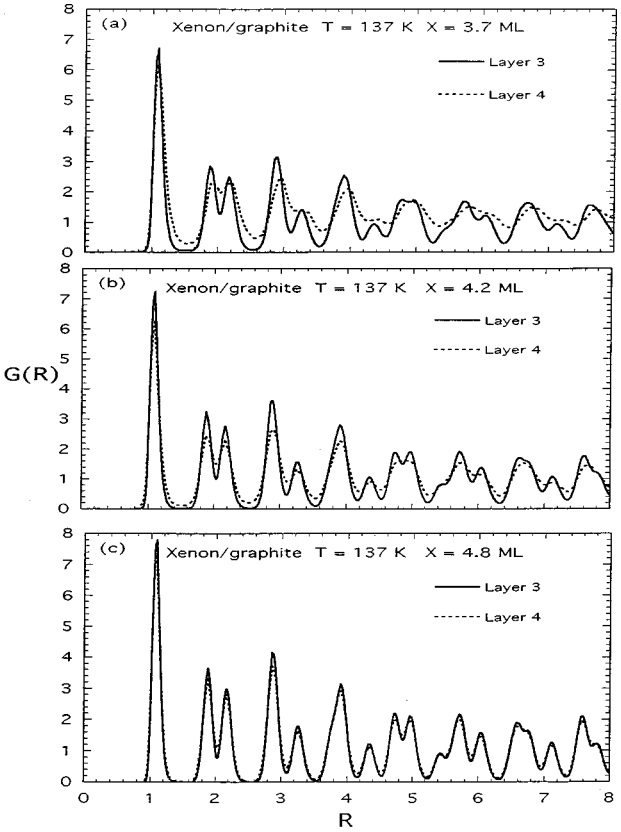

FIG. 8. Plots the 2D pair distribution functions ($T=137$ K) as the film passes through (Fig. 2) the 3 solid+1 fluid to the 4 solid+1 fluid regions. The change in bulk modulus [Eq. (6)] is computed to be 59 in this case. An indication of a sharp step is to be expected in the experiment. In Fig. 3 there is a final sharp peak in the compressibility consistent with the calculation.

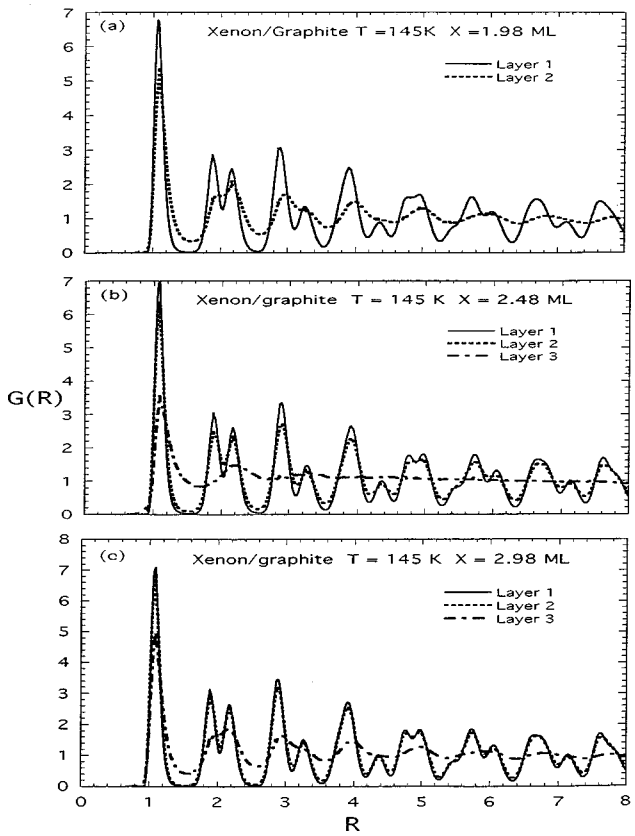

FIG. 9. Plots of our simulation results for the 2D pair distribution function for the individual layers in the film ($T=145$ K). (a) shows that the second layer is initially a full layer of liquid in the 1 solid+1 fluid region (Fig. 2). Layer 2 freezes just before (b). In (c) the third full layer of fluid has condensed. The change in the computed bulk modulus [Eq. (6)] from the film shown in (a) to (b) is 10. This is consistent with the low mounds in the experimental data (Fig. 5).

choice of coverages for display are the nearest we have to the onset and completion of a layering region. The coverages between those we report are qualitatively redundant. Figures 6–8 follow the coverage (not temporal) evolution of the xenon film as it grows from $1\frac{1}{2}$ to nearly five layers along the 137-K isotherm. Figure 6 shows the 2D pair distribution functions for the condensation of the second layer of xenon. In Fig. 6(a) the first layer is clearly a solid monolayer with a half layer of highly mobile fluid in the second layer. The second layer remains fluid up to nearly two full solid layers [Fig. 6(c)] when it sharply locks into a two-layer solid structure. This is typical of a vertical step in the isotherm and a large change in the compressibility (Fig. 3). This isotherm (137 K) crosses the sublimation region of the 2D phase diagram for the second layer. This is an example of the path-(a) type transition shown qualitatively in Fig. 1. The ensemble average for the bulk modulus through this region was the largest we observed and the experimental isotherm has the sharpest step.[16]

Figure 7 follows the film through the condensation and freezing of the third layer of the film. This two-step process is indicated in Fig. 2 to be passing from a two-solid+vapor to a two-solid+one-fluid region followed by the passage into a 3D-solid–vapor area. This would be a path-(c) crossing followed closely by a path-(d) type transition (see Fig. 1). This happens, as it should, at a slightly lower coverage than a typical solid-on-solid transition as occurred for layer 2. Structurally, this is not as easily resolved as the one-step process for layer 2. Graphic images of the top of the film easily distinguish between a 2D hypercritical fluid ($^iT > {}^iT_c$) and the 2D-vapor–2D-liquid coexistence phases ($^iT_t < T < {}^iT_c$). The triple and critical point temperatures of the ith layer are ^iT_t and ^iT_c, respectively. In the case of the 2D hypercritical fluid, the adsorbate atoms are more randomly distributed in an even density over the surface. In the 2D coexistence region for a layer, the graphic snapshots show the atoms coalescing into temporary islands, evaporating, and forming new islands. In the liquid-vapor coexistence case the experimental isotherms clearly show a round step followed by a kink. In Fig. 3 there are two experimental changes in compressibility and they are much lower. The simulation must rely on the quantitative calculation of the bulk modulus in these regions. Recall that the values for these two peaks were changes of 15 for the first layer and 12 for the second, in contrast to the 95 for layer 2. This strongly suggests that the film growth has crossed the 2D regions for a dense fluid to liquid followed by passage through the 2D solid-liquid coexistence zone. This realization is key to the understanding of how the isotherm steps first lose their sharp character.

At this point, the 137-K isotherm is three solid layers plus a very light 2D vapor in the fourth. As the film growth con-

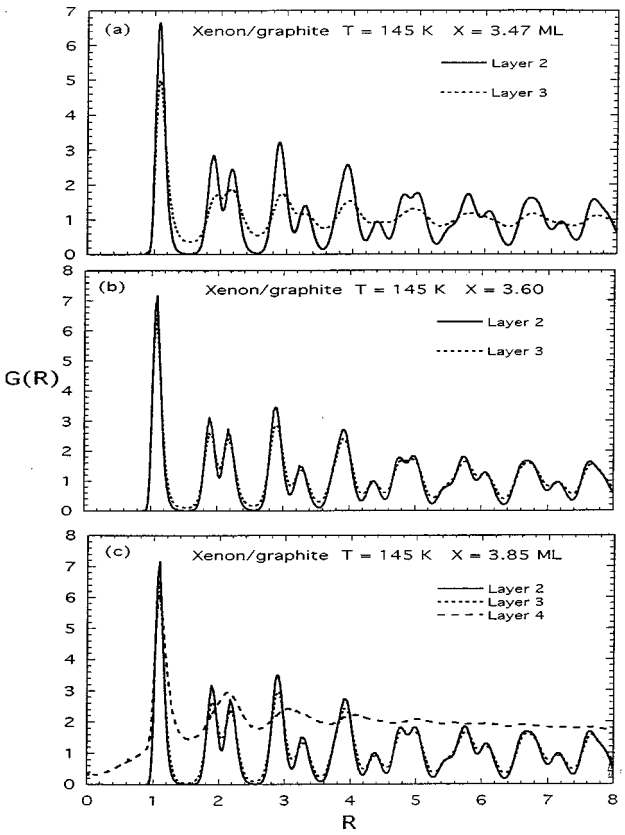

FIG. 10. Plots of our simulation results for the 2D pair distribution function for the individual layers in the film ($T=145$ K). (a)–(c) follow the film through the 2 solid+1 fluid to the 3 solid+1 fluid regions. The change in the computed bulk modulus [Eq. (6)] from the film shown in (a) to (b) is 41. This is consistent with the first sharp experimental peak in Fig. 5. (c) shows the liquid fourth layer on top of the film.

tinues, one layer of fluid is adsorbed, making nearly four layers. In the experiment (Fig. 3), this is shown by a ramp in the compressibility [a type-(c) path shown in Fig. 1]. Additional growth produces a striking resharpened or reentrant step. We suggest that this is a path-(a)-type (Fig. 1) solidification of the fourth step under a fifth layer of fluid. This is the start of the final three sharp steps seen in the experimental isotherms.[16,41] The first of these sharp steps is reflected in the compressibility (Fig. 3). In the simulation, the change in the bulk modulus across this step is 59, clearly more than the small changes in layer 3 but less than the 95 for layer 2. At this height, the substrate potential is significantly less. Figure 8 shows the 2D pair distribution functions for layers 3 and 4 as the growth increases from 3.7 to 4.8 layers. The fourth layer starts out as a modulated but mobile fluid. As the film thickness approaches nearly five full layers, the fourth layer freezes under the fifth layer, which is fluid. We believe that this scenario for the reappearance of sharp steps in experimental isotherms is an accurate depiction of this most interesting effect.

In the 145-K isotherm (Fig. 5), the reappearance of the sharp step occurs one layer thinner in the growth process. The behavior of the 2D pair distribution functions, the vertical distributions, and the bulk modulus computations should be consistent with the pattern we indicated for the 137-K isotherm. At this higher temperature, the second layer adsorbs as a 2D fluid (Fig. 9) at the coverage $X=1.98$ ML. At coverage 2.48 ML the second layer freezes [Fig. 1, path (d)]. The distinction from a path-(a) solidification comes from the small changes in the bulk modulus of 10. Layer 3 remains fluid until a coverage of 3.6 ML. The bulk modulus change between the coverages of 3.6 and those below is again large at 41. This indicates a path-(a)-type condensation of the third layer, but this time it is under a fluid in the fourth layer (Fig. 10). This higher-temperature change in bulk modulus is less than the one for the appearance of the sharp step in the 137-K isotherm (59), but still more than twice as large as the rounded step or kink-type isotherm features. The experimental data[41] in Fig. 5 show this step to be clearly sharper than the previous ones. The character of the layering is fundamentally different as the film passes from the two-solid+one-fluid to the three-solid+one-fluid regions of the phase diagram (Fig. 2). Again, the structure and bulk modulus combination from the simulation scales consistently with the derivatives of the experimental isotherm data. We believe this picture to be general and appropriate for the interpretation of the isotherm profiles over the ranges of temperature and coverage where the reentrant layering phenomena occur.

For the topside of thicker films, the influence of the substrate potential is progressively weaker. The layering transition lines are growing closer together and the details become indiscernible experimentally. Within a few layers the adsorption is merely the growth of bulk adsorbate solid from its own 3D vapor. This transitional change in growth behavior from film to bulk is an important point in the ongoing debate. Steps in the adsorption isotherms are resolvable in the most favorable cases for fewer than ten layers as a practical limit. In brief, the lattice-gas model[43] developed by den Nijs[20–22] and discussed by Weichman and co-workers[23,24] and Phillips and Larese[25] serves well in this preroughening region. The change in spreading pressure gradient flattens with height. The chemical potential approaches the value of that found for the equilibrium vapor pressure above the bulk. The heat capacity measurements by Zhu and Dash[5–8] and the diffraction profiles by Larese and co-workers[26,28,29] found the top of the film to be liquid when the temperature exceeds 80% of the bulk triple point. In the lattice-gas (RSOS) model by den Nijs, this ''fluid'' would not be described by a condensed 2D phase of mobile atoms (lattice sites are only filled or empty) but by the mobility of ''steps,'' i.e., a ''step liquid.'' The dynamical character of this surface model will be given in another paper.

It is appropriate to place the lattice model work with the scaling theory of Rommelse and den Nijs[20] and the mean-field effort by Weichman, Day, and Goodstein[23] in some context with our work on this problem. It is clear from the isotherm experiments that the ability to discern the steps and their nature becomes unresolvable before about ten layers. As the chemical potential is raised in the experiment it quickly approaches the bulk vapor pressure. At this point, one is essentially growing a bulk crystal front. In this region of the phase diagram (approximately ten layers or greater), the preroughening transitions proposed by den Nijs and coworkers are a good explanation for a solid-on-solid growth front. The Bruch criterion [Eq. (1)] cannot be met since the area per lattice site does not change in these models as practiced. A mathematically rigid lattice has no changing area, so

it has no change in compressibility. With no change in compressibility a discussion of the shape of the isotherm steps loses significance. On the (111) surface of a bulk crystal, this is not a problem. The lateral component of the compressibility is virtually constant. The existence of a layer or so of fluid on the surface of bulk need not exclude the preroughening model if one visualizes the mobile surface region as a step fluid rather than an atomic fluid. Viewing the adsorption isotherm as a monitoring of the changes in the compressibility of the film, the question of step profile becomes moot as the film thickness approaches the bulk and the compressibility approaches a constant.

From these considerations, we suggest that the progressive loss and reappearance of sharp steps in a physical adsorption isotherm is due to the details of the 2D phase diagram for each individual layer and the location of the crossing path on the phase diagram for that layer. The density differences of the coexisting phases in that particular crossing path leads to the magnitude of the change in the isothermal compressibilities. The larger the compressibility change, the sharper the step.

ACKNOWLEDGMENTS

We thank Marcel den Nijs, J. G. Dash, Aldo Migone, L. W. Bruch, Julius Hastings, and M. Lysek for helpful discussions. J.M.P. is grateful to the Department of Chemistry, Brookhaven National Laboratory for their hospitality. This work was supported by the U.S. Department of Energy, Material Science Division, under Contract No. DE-AC02-76CH00016.

[1] A. W. Adamson, *Physical Chemistry of Surfaces* (Wiley, New York, 1990).
[2] J. G. Dash, *Films on Solid Surfaces* (Academic, New York, 1975).
[3] W. A. Steele, *The Interaction of Gases with Solid Surfaces* (Pergamon, Oxford, 1974).
[4] J. S. Rowlinson and B. Widom, *Molecular Theory of Capillarity* (Clarendon, Oxford, 1982).
[5] D.-M. Zhu and J. G. Dash, Phys. Rev. Lett. **57**, 2959 (1986).
[6] D.-M. Zhu and J. G. Dash, Phys. Rev. B **38**, 11 673 (1988).
[7] D.-M. Zhu, Ph.D. thesis, University of Washington, 1988.
[8] D.-M. Zhu and J. G. Dash, Phys. Rev. Lett. **60**, 432 (1988).
[9] J. J. Hamilton and D. L. Goodstein, Phys. Rev. B **28**, 3838 (1983).
[10] J. J. Hamilton, Ph.D. thesis, California Institute of Technology, 1983.
[11] M. J. Lysek, Ph.D. thesis, California Institute of Technology, 1991.
[12] M. J. Lysek, M. LaMadrid, P. Day, and D. Goodstein, Langmuir **8**, 898 (1992).
[13] R. F. Hainsey, R. Gangwar, J. D. Shindler, and R. M. Suter, Phys. Rev. B **44**, 3365 (1991).
[14] R. Gangwar and R. M. Suter, Phys. Rev. B **42**, 2711 (1990).
[15] H. S. Youn and G. B. Hess, Phys. Rev. Lett. **64**, 918 (1990).
[16] H. S. Youn, X. F. Meng, and G. B. Hess, Phys. Rev. B **48**, 14 556 (1993).
[17] J. M. Phillips, Q. M. Zhang, and J. Z. Larese, Phys. Rev. Lett. **71**, 2971 (1993).
[18] M. T. Alkhafaji and A. D. Migone, Phys. Rev. B **45**, 8767 (1992).
[19] P. Day, M. Lysek, M. LaMadrid, and D. Goodstein, Phys. Rev. B **47**, 10 716 (1993).
[20] K. Rommelse and M. den Nijs, Phys. Rev. Lett. **59**, 2578 (1987).
[21] M. den Nijs and K. Rommelse, Phys. Rev. B **40**, 4709 (1989).
[22] M. den Nijs, Phys. Rev. Lett. **64**, 435 (1990).
[23] P. B. Weichman, P. Day, and D. Goodstein, Phys. Rev. Lett. **74**, 418 (1995).
[24] P. B. Weichman and D. Goodstein, Phys. Rev. Lett. **75**, 4331 (1995).
[25] J. M. Phillips and J. Z. Larese, Phys. Rev. Lett. **75**, 4330 (1995).
[26] J. Z. Larese and Q. M. Zhang, Phys. Rev. Lett. **64**, 922 (1990).
[27] G. B. Hess, in *Phase Transitions in Surface Films 2*, edited by H. Taub *et al.* (Plenum, New York, 1991), pp. 367–389.
[28] J. Z. Larese *et al.*, Phys. Rev. B **40**, 4271 (1989).
[29] J. Z. Larese, Acc. Chem. Res. **26**, 353 (1993).
[30] L. W. Bruch, J. Unguris, and M. B. Webb, Surf. Sci. **87**, 437 (1979).
[31] L. W. Bruch and M. S. Wei, Surf. Sci. **100**, 481 (1980).
[32] M. S. Wei and L. W. Bruch, J. Chem. Phys. **75**, 4130 (1981).
[33] J. M. Phillips, Phys. Rev. B **34**, 2823 (1986).
[34] R. L. Elgin, Ph.D., California Institute of Technology, 1973.
[35] M. Bretz, J. G. Dash, D. C. Hickernell, E. O. McLean, and O. E. Vilches, Phys. Rev. A **8**, 1589 (1973).
[36] M. Bretz, J. G. Dash, D. C. Hickernell, E. O. McLean, and O. E. Vilches, Phys. Rev. A **9**, 2814 (1974).
[37] Y. Larher, J. Chem. Soc. Faraday Trans. I **70**, 320 (1974).
[38] A. Thomy and X. Duval, J. Chim. Phys. **67**, 1101 (1970).
[39] A. Thomy and X. Duval, J. Chim. Phys. **66**, 1966 (1969).
[40] P. Day, M. LaMadrid, M. Lysek, and D. Goodstein, Phys. Rev. B **47**, 7501 (1993).
[41] Q. M. Zhang and J. Z. Larese, Phys. Rev. B **52**, 11 335 (1995).
[42] H. S. Youn, X. F. Meng, and G. B. Hess, Phys. Rev. B **48**, 14 556 (1993).
[43] T. L. Hill, *Statistical Mechanics* (McGraw-Hill, New York, 1956).